Study on heat transfer performance of ultra-low temperature radiant heating modules

Dong GUANG[a], Jiabin WANG, Huiyao GAO[b], Mengyuan LI[b],Luhan CAO[b], Huifan ZHENG[b]*

a Henan Mechanical and Electrical Vocational College, Zhengzhou, 451192, China;

b School of Energy and Environment, Zhongyuan University of Technology, Zhengzhou 451191, China

Abstract:*To address the low energy efficiency of renewable energy, the high water supply temperature, and the high power consumption of pumps, this paper propose an assembled capillary radiant heating floor based on solar collector heating and analyze its heat transfer performance.It is found that the capillary tube layout using the I-type laying method is more uniform than the U-type laying method , and the overall temperature is higher. And the narrower the pipe spacing is, the greater influence on the floor surface average temperature is. For type I paving, the optimal main pipe supply flow range is 0.2 ~ 0.25m/s, and the optimal water supply temperature range is 32℃~36℃. Through the orthogonal test analysis of U-type floor, the results show that the variance S of the corresponding water supply temperature is 9.59, while the S value of the corresponding water supply velocity is only 0.03.In both I-type and U-type paving methods, the influence of water supply temperature is greater than water supply flow rate on the thermal performance of the floor.*

Keywords: *Ultra-low temperature radiant heating; Assembled floor; Orthogonal test design; Numerical simulation; Thermal performance*

1.Introduction

The construction industry accounts for 23% of CO_2 emissions from global economic activities, of which China accounts for nearly 41%[1]. According to the report of the International Energy Agency, with the energy standards and equipment of zero-carbon buildings becoming more and more advanced, even if the heating area increases by 30%, the heating energy consumption of building space can be reduced by nearly 70%.Therefore, selecting energy-efficient cooling and heating solutions will be highly important for conserving energy, reducing emissions, and promoting the green transformation of industry.

Compared to other heating methods like air conditioning and radiators, low-temperature hot water radiant floor heating offers significant advantages [3]. Ala Hasan et al. [4]found that integrating a low-temperature water heating system with radiant floors significantly enhances comfort compared to conventional radiators and underfloor heating systems. Kassim MS et al. [5]noted that compared with the traditional radiator heating method, the low-temperature radiant floor heating system can

save 20% to 30% energy.[6]. Additionally, advancements in modular construction materials have made the assembly of radiant floor modules an effective solution to the issues faced by traditional heating systems[7]. Silva et al. explored optimization strategies for modular buildings using simulation and calculation software, achieving designs that aim for zero energy consumption [8]. O'Pons et al. investigated the energy consumption and environmental impacts of over 200 schools in Spain, finding that modular assembled buildings consume less energy and produce less waste compared to traditional cast-on-site construction [9].

Capillary heat exchangers present a viable alternative to traditional radiators and electric heaters when paired with heat pumps due to their expansive surface area and lower operating temperatures[10]. Compared to conventional air conditioning systems, capillary ceiling radiant cooling wall panel (CCRCP) systems are known for their low energy consumption, reduced noise levels, and enhanced indoor thermal comfort[11], and both radiant cooling and radiant heating technologies are suitable for low-load environment[12]. With equal water supply temperatures, capillary tubes provided a more uniform surface temperature distribution [13]. Roof heating efficiency was 4.36% higher than floor heating, but radiant floor heating achieved better surface temperature stability, more uniform temperature distribution, and improved comfort[14]. Many scholars have studied the influencing factors of radiation characteristics of unassembled capillary tubes.Tomas Mikeska et al. analyzed the radiant heat transfer dynamics of capillary tube systems, focusing on the effects of filling layer thickness and water temperatures on capillary tube wall temperatures[15]. Pei Ding et al. investigated factors influencing floor thermal performance, noting that heat dissipation decreases as the distance between tubes increases, with this effect determined by the equivalent distance between tubes [16]. Wei Xinli et al. conducted simulations to explore factors affecting surface temperature and heat dissipation in floors of air source heat pump systems. They found that the material and physical properties of the floor's decorative layer had the most significant impact on temperature uniformity, followed by pipe spacing, with internal filling layer thickness having the least effect [17]. Wang Xin and Li Longxin combined theoretical and numerical analyses to assess how varying water supply conditions and floor structural design parameters affect surface temperature distribution and heat flow density in radiant heating systems using air source heat pumps[19]. Taeyeon et al. constructed and simulated a capillary radiant cooling air-conditioning system, reporting a 27% reduction in power consumption and 30% less energy usage compared to all-air systems[21]. Fu et al. studied the thermal transfer characteristics of capillary radiant heating floors, developed a glow temperature model, and analyzed various factors affecting heat transfer, offering theoretical insights for radiant floor heating systems[24].

The heat source temperature for low-temperature radiant floor heating systems typically ranges from 35 to 50℃. Considering human comfort standards, many studies suggest maintaining the water supply temperature close to 35℃. Conventional radiant floor systems, which use plastic tubing, often have high thermal resistance. If the water supply temperature is not sufficiently low, using low-grade heat sources can diminish energy efficiency. To address this, radiant floor heating systems can be enhanced by integrating solar collectors, which provide a low-temperature heat source and improve overall efficiency. The utilization of low-grade energy has been extensively researched for providing high-temperature domestic hot water, such as the use of novel solar-biomass hybrid systems (HSBS) in buildings to produce domestic hot water at 60℃ for space heating[25], and the design of concentrated solar power towers for hot water heating [26]. The use of solar water heaters (SWH)

and solar air heaters (SAH) will greatly contribute to environmental protection and sustainable economies[27]. Hu D et al. designed an indirect solar thermal hot water system based on a rural area in Shenyang, and found that the technical and economic performance of the air source heat pump-assisted solar water system was significantly improved compared to other heating methods[28]. Pinamonti, M, and others conducted energy simulations to evaluate the system's performance, demonstrating that the solar energy utilization rate increased by about 5% after adding a heat pump compared to a solar energy system without a heat pump [29]. Some scholars have used solar thermal systems to provide space heating and domestic hot water for research houses, and found that the annual energy storage efficiency of seasonal energy storage tanks is 42%[30] , and the solar energy utilization rate can exceed 90% [31].

In summary, while numerous domestic and international studies have explored the heat transfer characteristics of radiant floor air conditioning systems, most research has concentrated on large-area radiant floor structures. There is a gap in the investigation of factors affecting the heat transfer performance of assembled capillary radiant floor cooling/warming systems under operational conditions. In order to solve this problem, this paper introduces an assembled capillary ultra-low temperature radiant floor which can use solar hot water, and analyzes the heat transfer performance of two capillary structures.

2. Establishment of model

As shown in Fig. 1, the internal structure of the assembled capillary low-temperature radiant floor consists, from bottom to top, of an insulation layer, a reflective layer, a concrete filling layer with embedded capillary tube network, a leveling layer and a decorative layer. The insulation layer is made of expanded polystyrene (EPS) board covered by a vacuum aluminized film, which reduces downward heat loss and enhances upward heat reflection. The filling layer is a 40 mm thick concrete layer in which the capillary tube network made of PPR plastic pipes (20×2 mm main pipes and 4.8×0.8 mm capillary tubes) is fixed by a wire mesh, providing heat storage and transferring heat relatively uniformly to the floor surface. Above it, a 15 mm thick cement mortar leveling layer ensures a flat base for the finishing material, and the outermost layer is an approximately 5 mm thick ceramic tile decorative layer with good thermal conductivity, long service life and favourable economic performance，as shown in Fig. 1.

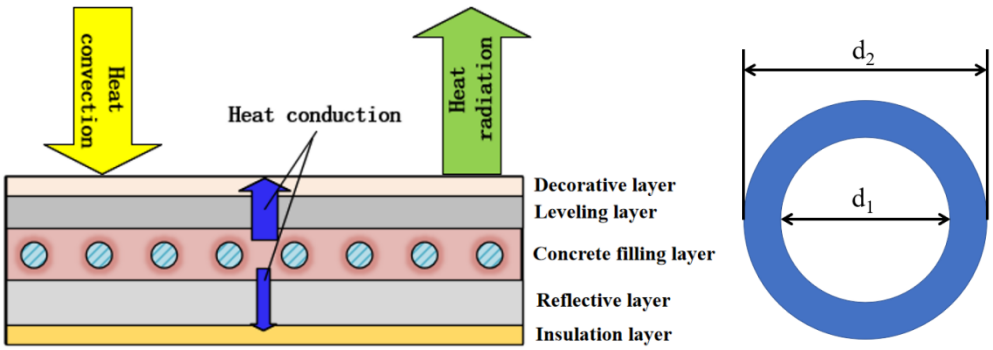

Fig. 1 Schematic diagram of internal structure form and capillary structure of floor

As illustrated in Fig. 1, the low-temperature hot water heats the inner wall of the capillary tube through forced convection. This heat is then conducted through the capillary wall, filling layer, leveling layer, and decorative layer. The radiant heating process between the floor surface and the

indoor environment involves both radiation and convection, with radiation being the dominant mode. The floor surface radiates heat to other non-heating surfaces via thermal radiation.

The simulation in this study focuses on fluid flow and heat transfer, governed by the following three fundamental control equations:

（1）Mass conservation equation

$$\frac{\partial \rho}{\partial t} + \frac{\partial}{\partial x_i}(\rho u_i) = S_m \quad (1)$$

Where ρ is the density, kg/m^3; u is the velocity, m/s. The source term S is the mass added to the continuous phase from the dispersed secondary phase.

（2）Momentum conservation equation

$$\frac{\partial}{\partial t}(\rho u_i) + \frac{\partial}{\partial x_j}(\rho u_i u_j) = -\frac{\partial p}{\partial x_i} + \frac{\partial \tau_{ij}}{\partial x_j} - \rho g_i + F_i \quad (2)$$

$$\tau_{ij} = \left[\mu\left(\frac{\partial u_i}{\partial x_j} + \frac{\partial u_j}{\partial x_i}\right)\right] + \frac{2}{3}\mu \frac{\partial u_l}{\partial u_l}\delta_{ij} \quad (3)$$

Where p is pressure, pa; μ is the dynamic viscosity, kg/(m • s); g_i and F_i are the gravitational volume force and the external volume force acting in the I-direction, $F_i$contains other model-related source terms, N.

(3) Energy conservation equation

$$\frac{\partial(\rho T)}{\partial t} + div(\rho u T) = \left(div \frac{k}{c_p} grad T\right) + S_T \quad (4)$$

Where c_p is the heat capacity, J/(kg k); T is temperature, K; S_T is the internal heat generation within a fluid, as well as the mechanical energy that is converted into thermal energy as a consequence of viscous forces.

The plane size of the assembled radiant floor model needs to meet the requirements of the 3 M modulus, and the length and width dimensions can be 600×300 mm, 900×600 mm, and 1200×900 mm.The assembled capillary radiant floor is manufactured as standardized prefabricated modules, and its in-plane dimensions are specified using modular coordination on a 3M modular grid. According to the modular coordination standard (basic module M = 100 mm), commonly used module sizes in engineering practice include 600 × 300 mm (6M × 3M), 900 × 600 mm (9M × 6M), and 1200 × 900 mm (12M × 9M). In this study, the 600 × 300 mm (6M × 3M) module is selected as a representative unit because it aligns with widely used prefabricated products and installation procedures while substantially reducing the computational cost for orthogonal-design parametric runs; in practical applications, a room-scale floor is formed by assembling multiple modules, and the heat-transfer behavior in interior regions away from edges is dominated by local structure and operating conditions, so the module-level results can be regarded as representative of the assembled floor system.The assembled capillary low-temperature radiant floor studied in this paper uses U-type and I-type (as shown in Fig. 2) forms; the U-type model has a same-side return, while the I-type model has an opposite-side return. The overall size of the radiant floor is 600×300 mm, with capillary tube spacings of 10 mm, 20 mm, and 30 mm. The model is constructed as depicted in Fig. 2.

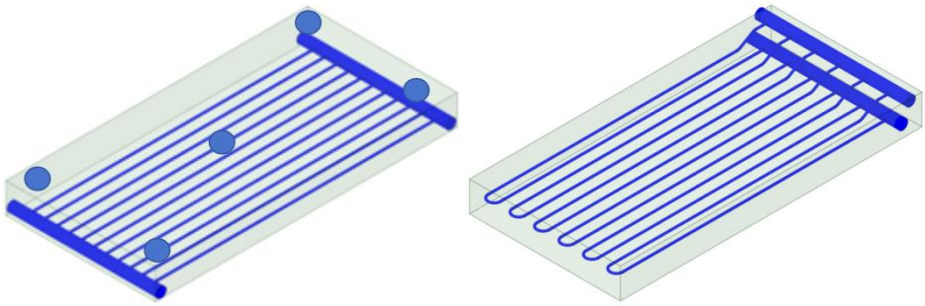

Fig. 2 Schematic diagram of I (left) and U (right) models

3. Result analysis of floor heat transfer performance

3.1Grid Segmentation and Model Assumptions

The following assumptions are made for the assembled capillary radiant floor model to improve computational efficiency:

(1) All sides and bottom of the floor are regarded as thermal insulation surfaces;

(2) Ignore all wall thermal resistances.

(3) The various materials are regarded as incompressible, and their physical parameters are constants.

Since the model in this study is more complex and has many meshes, a polyhedral mesh (Poly) is used, ANSYS Mesher is utilized for meshing, and the meshing results are shown in Fig. 3. The grids around the capillary tubes are small and dense in order to capture the strong temperature and velocity gradients.

In ANSYS Fluent, a three-dimensional segregated transient solver was adopted. The energy equation was activated to solve the heat transfer in both the fluid and solid regions. The k–ω turbulence model was used to describe the viscous effects of the flow inside the capillary tubes. In addition, the Solidification/Melting model available in Fluent was enabled. These numerical settings were used for all simulation cases in this study.

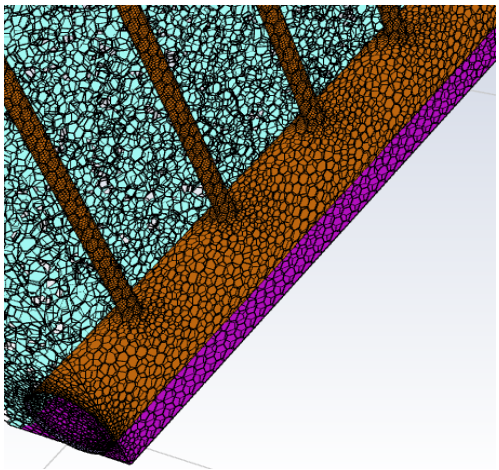

Fig. 3 Assembled capillary radiation heating floor grid

3.2 Boundary condition setting

The model is divided into solid domain and fluid domain. The fluid domain is the low-temperature hot water in the capillary, and the solid domain is the capillary wall and equivalent packing layer. The physical parameters of low-temperature hot water in fluid domain are set as density of 1000kg/m^3, heat transfer coefficient of 0.599 W/(m·K) and specific heat capacity of 4200 J/(kg·K). Relevant boundary conditions and parameters are set, as shown in Tab. 1.

Tab. 1 Related boundary conditions

Name	Boundary condition type	Parameter setting
Heating pipe entrance	Velocity Inlet	Velocity：0.3m/s Temperature：308K
Heating pipe outlet	Pressure Outlet	——
Upper surface of floor	Mixed boundary	Convective heat transfer coefficient：7W/m^2·K Radiance of surface：0.75 External radiation temperature：289K
Under surface of floor	Adiabatic wall	heat flux：0
Side surface of floor	Adiabatic wall	heat flux：0

3.3 Model reliability verification

In this work, five representative points are selected on the surface of the 600×300 mm radiant floor for model verification, as shown in Fig.2 (left). These points are located at the four corners and at the centre of the plate. According to Eqs. (1) – (4), the surface temperatures at these locations are obtained analytically and compared with the numerical results, as illustrated in Fig.4.The relative errors at the five points are all within 3%, which demonstrates that the present model has satisfactory calculation accuracy.

It should be noted that the present study mainly focuses on numerical analysis and that full-scale experimental validation of the assembled capillary radiant floor has not yet been completed. Nevertheless, the magnitude of the surface temperatures and their variation trends with operating parameters predicted by the model are consistent with the ranges reported in previous experimental studies on capillary radiant floor and roof systems [14 – 18,24]. These experimental results provide indirect evidence for the physical soundness of the present numerical model. In future work, a dedicated full-scale test rig of the assembled capillary radiant floor will be constructed to measure surface temperature distributions and heat fluxes under controlled operating conditions, so that more detailed comparisons between measured data and numerical predictions can be carried out.

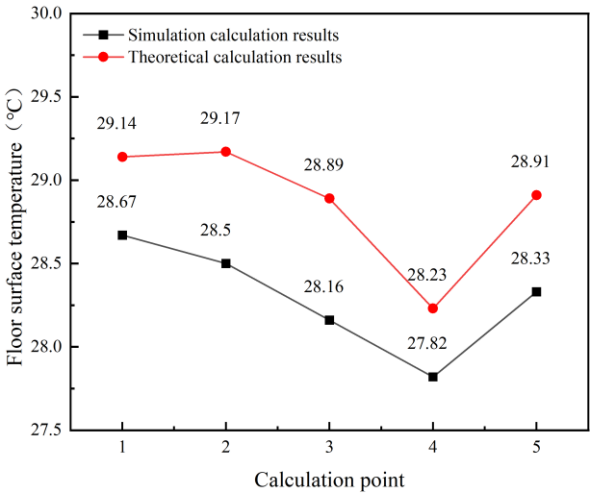

Fig. 4 Simulation result verification

3.4 Thermal performance analysis of floor under different structural parameters

When the inlet temperature of the main pipe is 35℃, the water flow rate of the main pipe is 0.3 m/s, and the distance between branch pipes is 20 mm, the effects of different methods of laying capillary tubes on heat transfer performance were studied. In comparing the U-type and I-type capillary tube laying methods, the temperature distribution of heating floor are shown in Fig. 5. The two laying methods of the floor surface of the highest temperature areas are present in the supply and return of water where the main location is located. Compared with the U-type paving method, the capillary tubes using the I-type paving method result in a more uniform floor surface temperature distribution. The U-type paving method results in a high temperature at one end of the end of the low-temperature effect, whereas the I-type paving methods of the two supply and return mains are distributed at the two ends of the floor. Thus, the floor temperature is more uniform, and the floor surface temperature of the lowest temperature region appears on the left side of the floor. By analyzing the temperature in the middle area of the floor surface, it is found that the U-shaped paving mode is 27.82℃, and the I-shaped paving mode is 28.33℃, which is about 0.51℃ higher than the U-shaped paving mode.These findings indicate that the thermal conduct performance of I-type tube laying method is better than that of the U-type laying method.

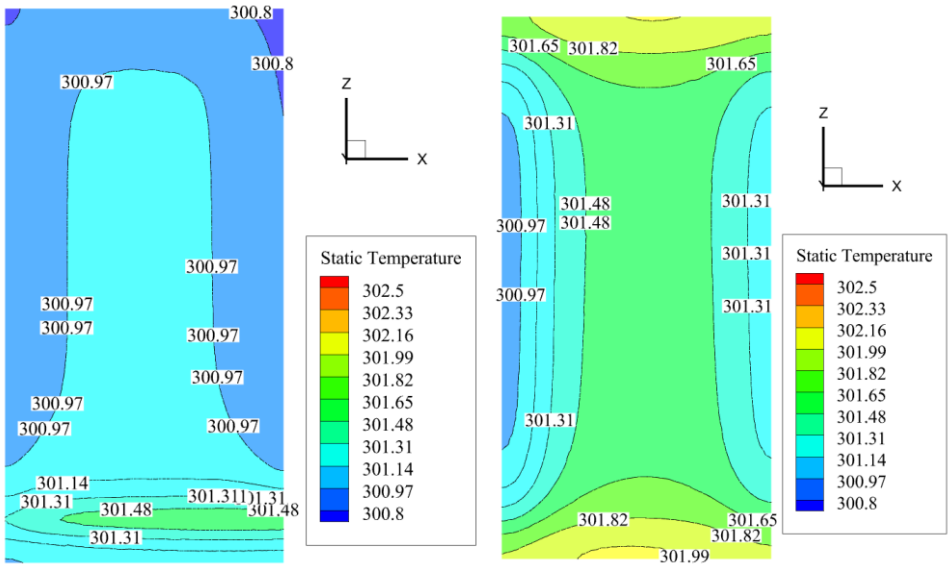

Fig. 5 Comparison of simulated surface temperatures of floors with U-type (left) and I-type (right) laying methods

To study the effects of different capillary tube spacings on thermal conduct performance of floor, an I-type capillary radiation floor model was used, with a inlet water temperature of 35℃ and a main pipe water flow rate of 0.3 m/s under working conditions. Compared with the 10 mm, 20 mm, and 30 mm tube spacing conditions,the results of the cloud maps are shown in Fig. 6. Judging from the uniformity of temperature distribution on the floor surface, the tighter the tube spacing is, the more uniform the distribution of the floor surface temperature. By analyzing the surface average temperature in the middle area of the floor, it is found that the temperature of pipe spacing of 10mm is 0.68℃ higher than that of pipe spacing of 20mm, and the average temperature of pipe spacing of 20mm is 0.34℃ higher than that of pipe spacing of 30mm, which shows that the smaller the pipe spacing, the greater the influence on floor surface average temperature.

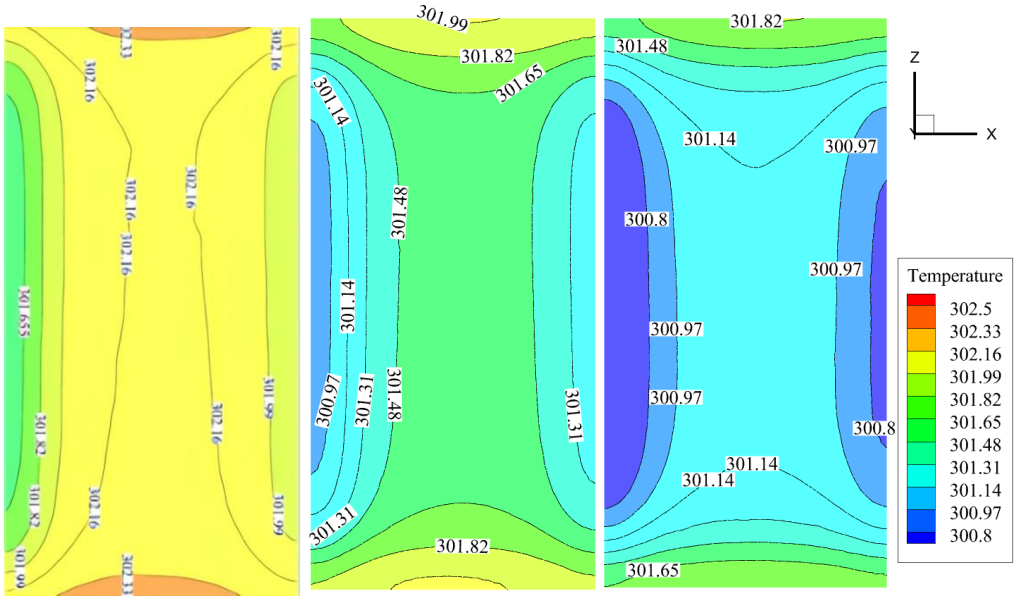

Fig. 6 Comparison of floor temperatures at 10mm (left), 20mm (center) and 30mm (right) tube spacing.

3.5 Thermal performance analysis of I-shaped floor

Under the working condition of a inlet water temperature of 35℃, the trends of surface average temperature change in I-type model with pipe spacings of 10 mm, 20 mm and 30 mm were compared and analyzed under five different main pipe water supply flow rates, as shown in Fig. 7. With the increase of flow rate, the gradient value of the floor surface average temperature elevation gradually increases. Comparing the average temperature of the floor surface with three kinds of pipe spacing, it is found that the temperature rise is the most obvious when the flow rate is between 0.2m/s and 0.25 m/s. Among them, 0.1℃ is increased at 10mm tube spacing; Increase 0.05℃ at 20mm tube spacing; Increase 0.03℃ at 30mm tube spacing. When the water flow rate increases from 0.25m/s to 0.3m/s, the gradient of surface temperature rise decreases.

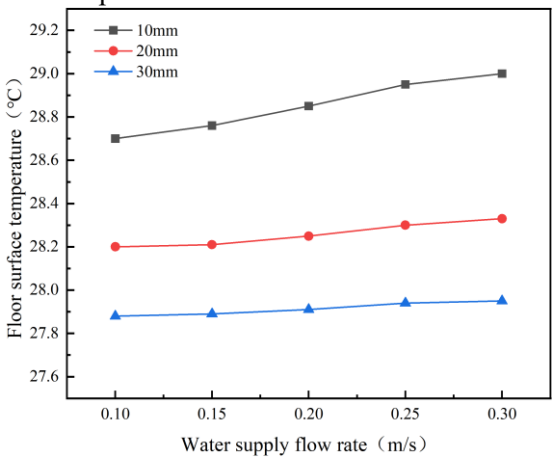

Fig. 7 Variation diagram of floor temperature under the influence of different water supply flow rates

When the main pipe water flow rate is 0.3 m/s, the trends of floor surface average temperature changes in seven water supply temperatures of I-type models with three pipe spacings were compared and analyzed, as shown in Fig. 8. By studying surface average temperature, it is found that the temperature rises gently in the range of 31℃ to 32℃, and the gradient value of temperature rise in the range of 32℃ to 36℃ is gradually increasing.The optimal water supply temperature is between 33℃ and 34℃ under the condition of 10mm pipe spacing, and the average floor temperature in the interval increases by 0.9℃.The optimal water supply temperature is between 32℃ and 33℃ with 20mm pipe spacing and 30mm pipe spacing, and the floor surface average temperature in the interval increases by 0.8℃ and 0.76℃ respectively. When the inlet water temperature exceeds 36℃, the curve of the upward trend slightly flattens.

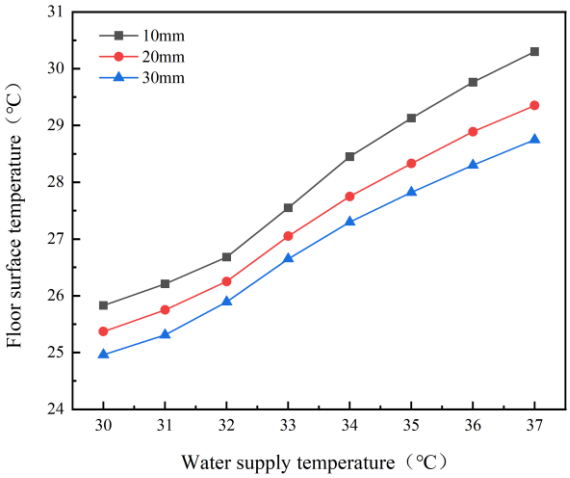

Fig. 8 Variation diagram of floor temperature under the influence of different inlet water temperature

The above analysis illustrates that surface average temperature is more affected by changing the inlet temperature than by changing the flow rate for same pipe spacing.

3.6 Performance analysis of U-shaped floor

After the simulation and verification analysis of I-type assembled low-temperature radiant heating floor model, three U-type assembled capillary low-temperature radiant heating floor models with different pipe spacing are established respectively. The physical parameters, boundary conditions and calculation methods of the model are all set at the original values, and then we simulate different water supply conditions.

In the orthogonal test design for the U-type floor, three levels were selected for each factor based on practical operating ranges and product constraints of ultra-low-temperature capillary radiant floor systems. The inlet water temperatures of 31 °C, 33 °C and 35 °C represent typical low, medium and high values within the ultra-low-temperature regime that can be achieved by solar collector–assisted heat pump systems, and are consistent with recommended supply temperatures for low-temperature radiant floor heating [3,14,24]. The main pipe velocities of 0.1, 0.2 and 0.3 m/s cover the feasible operating range of the circulation pump used in this study and correspond to low, nominal and high flow conditions. The capillary tube spacings of 10, 20 and 30 mm reflect compact, standard and relatively sparse layouts, respectively, which are compatible with the geometric constraints of commercial capillary modules [15–18]. Therefore, the chosen factor levels provide a representative design space for evaluating the thermal performance and sensitivity of the assembled capillary radiant floor.

Simulate and calculate the 9 working conditions in Tab. 2 respectively, and the results are shown in the following table:

Tab. 2 Simulation calculation results

Factor level / Serial number	Inlet temperature, Inlet velocity, Tube spacing	Average temperature of floor surface/℃
1	31℃，0.1 m/s，10 mm	26.15
2	31℃，0.2 m/s，20 mm	25.55
3	31℃，0.3 m/s，30 mm	25.38
4	33℃，0.1 m/s，20 mm	26.92
5	33℃，0.2 m/s，30 mm	26.65
6	33℃，0.3 m/s，10 mm	27.55
7	35℃，0.1 m/s，30 mm	27.88
8	35℃，0.2 m/s，10 mm	28.96
9	35℃，0.3 m/s，20 mm	27.82

It is assumed that the index Y analyzed in this test represents that the surface average temperature of the assembled capillary radiation floor is 25℃ different from the design temperature of the floor surface. By calculating and analyzing the range and variance, the simulation results are sorted out. Relevant parameters and formulas in the table are as follows:

$$P = J_1^2 + J_2^2 + J_3^2 \tag{5}$$

$$M = P/3 \tag{6}$$

$$S = M - K \tag{7}$$

$$G = Y_1 + Y_2 + Y_3 + Y_4 + Y_5 + Y_6 + Y_7 + Y_8 + Y_9 \tag{8}$$

$$K = G^2/9 \tag{9}$$

$$Y = G/9 \tag{10}$$

Where J1, J2 and J3 are the sum of the analysis indexes corresponding to the three columns of numbers A, B and C;S is the variance;R is the range;J1, J2 and J3 are the differences between the maximum and minimum values of the average values of test indexes.According to Formulas（5）~（10）, the analysis results shown in the following table can be obtained.

Tab. 3 Result analysis

Working condition	A	B	C	Analysis index Y_i
1	1	1	1	1.15
2	1	2	2	0.55
3	1	3	3	0.38
4	2	1	2	1.92
5	2	2	3	1.65
6	2	3	1	2.55
7	3	1	3	2.88
8	3	2	1	3.96
9	3	3	2	2.82

Tab. 4 Detailed indicator results

Analysis index	A	B	C
J_1	2.08	5.95	7.66
J_2	6.12	6.16	5.29
J_3	9.66	5.75	4.91
P	135.1	106.41	110.77
M	45.03	35.47	36.92

R	2.53	0.14	0.92
S	9.59	0.03	1.48

According to the calculation results of variance s value in Tab. 4, it is evident that inlet temperature exerts the greatest influence on the surface average temperature of the assembled capillary temperature radiant heating system. The spacing between capillary tubes has the next most significant impact. In contrast, the main pipe supply velocity shows a minimal effect on the surface average temperature, with an S value of only 0.03. Additionally, the range r value calculations confirm that the factors affecting the floor surface temperature, in descending order of influence, are: water supply temperature, capillary tube spacing, and water flow rate .

By analyzing the calculation results of the floor surface average temperature corresponding to the above nine working conditions, it is found that the design value of the floor surface average temperature of 25℃ is met with low-temperature hot water of 31℃ in the third working condition.

4. Conclusion

In our study, we analyzed the principles of radiant floor heating and developed two simulation models for assembled floor radiation. We examined the heat transfer characteristics of floors with U-shaped and I-shaped pipe layouts. We assessed the impact of pipe spacing, water flow rate, and water supply temperature on the heat transfer of the I-shaped assembled floor.

(1) It was found that the two types of laying methods for the floor surface of the highest-temperature region appeared in the supply and return main locations. Additionally, the capillary tubes using the I-type laying method provided more uniform floor surface temperature distribution than the U-type laying method, and the temperature was higher.

(2) In the middle section of the floor, a tube spacing of 10 mm resulted in a average surface temperature 0.68℃ higher than that with a 20 mm spacing, while the 20 mm spacing was 0.34℃ higher than a 30 mm spacing. This shows that reducing the tube spacing significantly improves the floor surface temperature.

(3) Both the I-type and U-type flooring systems demonstrate that the temperature of the water supply exerts a more substantial influence on thermal efficiency than the water flow velocity. For I-type layout, the most effective water flow rate is between 0.2 to 0.25 m/s, while the ideal water supply temperature is between 32℃ and 34℃.

(4) In future work, a full-scale prototype of the assembled capillary radiant floor will be constructed and instrumented in a laboratory test room and in selected buildings. Long-term measurements of surface temperature, heat flux and indoor thermal comfort will be carried out under different operating conditions, so as to further validate the numerical model and comprehensively evaluate the seasonal energy-saving potential and practical applicability of the proposed system.

Acknowledgement

This work was supported by the National Natural Science Foundation of China (No.52476023), the Key Research Program of Higher Education Institutions in Henan Province (No.24A470014), and the Special Key Research and Development Program of Henan Province (No. 231111320900), China Textile Industry Federation Science and Technology Guidance Plan Project (No.2024021).

References

[1]. Guo F ,Wang J ,Song Y .Reducing carbon emissions in prefabricated buildings supply chains: a focus on component manufacturing processes.[J].Environmental science and pollution research international,2024,34507-34525.

[2]. Wang S ,Li C ,Zhang W , et al.Assessing the impact of prefabricated buildings on urban green total factor energy efficiency[J].Energy,2024,297131239-.

[3]. Zhang C, Michal P. A review of integrated radiant heating/cooling with ventilation systems-Thermal comfort and indoor air quality[J]. Energy & Buildings, 2020, 223(110094):1-18.

[4]. Ala Hasan,Jarek Kurnitski,Kai Jokiranta.A combined low temperature water heating system consisting of radiators and floor heating[J].Energy and Buildings.2009(41), p470–479.

[5]. Kassim MS,S.KM,A.AI,et al.Experimental and Numerical Study of Radiant Floor Heating Panels Performance at Different Conditions[J]. Iop Conference Series: Materials Science and Engineering,2020(1).

[6]. Wenye L, Zhenjun M, M. I S, et al. Development and evaluation of a ceiling ventilation system enhanced by solar photovoltaic thermal collectors and phase change materials[J]. Energy Conversion and Management, 2014,88.

[7]. Wang T.Study on Thermal Performance of Prefabricated Low Temperature Radiantheating floor[D].Dissertation for the Master Degree,Hunan University of Technology,Zhuzhou prefecture level city,2020.S.Pedro C.P,A.Manuela,B.Luís,et al. Development of prefabricated retrofit module towards nearly zero energy buildings,Energy & Buildings.56.(2013):115-125.

[8]. Silva P C P, Almeida M, Bragança L, et al. Development of prefabricated retrofit module towards nearly zero energy buildings[J]. Energy & Buildings, 2013,56:115-125.

[9]. Pons O, Wadel G. Environmental impacts of prefabricated school buildings in Catalonia[J]. Habitat International, 2011,35(4):553-563.

[10]. Valters D ,Jevgenijs T ,Andris J .Thermal Comfort in Indoor Spaces with Radiant Capillary Heaters[J].Environmental and Climate Technologies,2022,26(1):708-719.

[11]. Gang P ,Linghong X ,Qiming Y , et al.Load Prediction and Control of Capillary Ceiling Radiation Cooling Panel Air Conditioning System Based on BP Neural Network[J].IOP Conference Series: Earth and Environmental Science,2021,769(4):

[12]. Miriel J, Serres L, Trombe A. Radiant ceiling panel heating-cooling systems: experimental and simulated study of the performances, thermal comfort and energy consumptions[J]. Applied thermal engineering: Design, processes, equipment, economics, 2002,22(16):1861-1873.

[13]. Cho J, Park B, Lim T. Experimental and numerical study on the application of low-temperature radiant floor heating system with capillary tube: Thermal performance analysis[J]. Applied Thermal Engineering, 2019,163(C).

[14]. Zou H, Long E, Zhang Y, et al. Experimental study on thermal performance of roof and floor capillary radiant heating system[J]. IOP Conference Series: Earth and Environmental Science, 2019,310(3):32075.

[15]. Mikeska T, Svendsen S. Study of thermal performance of capillary micro tubes integrated into the building sandwich element made of high performance concrete[J]. Applied Thermal Engineering, 2013,52(2):576-584.

[16]. Ding P, Li Y, Long E, et al. Study on heating capacity and heat loss of capillary radiant floor heating systems[J]. Applied Thermal Engineering, 2020,165(C):114618.

[17]. Wang L, Shang S. Research Status and Progress of Air Source Heat Pump Direct Floor Radiant Heating System[J]. Construction And Budget, 2019(03):31-34.

[18]. Wei X, Zhang F, Jian S, et al. Simulation and optimisation of radiant floor heating with refrigerant R22 as work mass[J]. Journal of Zhengzhou University (Engineering Science), 2011,32(02):6-9.

[19]. Wang X. The Effect Analysis and Research of Direct Floor Radiant Heating with Air Source Heat Pump[D].Dissertation for the Master Degree, Hebei University Of Science And Technology, 2014.

[20]. Li L.Study on The Heat Transfer and Operation Characteristics of Air SourceHeat Pump Direct Condensing Floor Radiant Heating System[D]. Dissertation for the Master Degree, Shenyang Jianzhu University, 2018.
[21]. Shuzo M, Shinsuke K, Taeyeon K. Coupled simulation of convicton, radiation, and HVAC control for attaining a given PMV value[J]. Building and Environment, 2001,36(6).
[22]. Corina S. Energy and peak power savings potential of radiant cooling systems in US commercial buildings[J]. Energy & Buildings, 1999,30(2).
[23]. Taeyeon K, Shinsuke K, Shuzo M. Indoor cooling/heating load analysis based on coupled simulation of convection, radiation and HAVC control[J]. Building and environment, 2001,36(7).
[24]. Shenghua F ,Yang P ,Xingping W , et al.Numerical Simulation of Heat Transfer Characteristics of Capillary Radiant Heating Floor[J].KSCE Journal of Civil Engineering,2024,28(2):546-556.
[25]. Krarouch M ,Allouhi A ,Hamdi H , et al.Energy, exergy, environment and techno-economic analysis of hybrid solar-biomass systems for space heating and hot water supply: Case study of a Hammam building[J].Renewable Energy,2024,222119941-.
[26]. Mohamed Q ,S. H E ,Junfeng W , et al.Design and thermal performance analysis of concentrating solar power tower for water heating systems[J].Case Studies in Thermal Engineering,2023,48
[27]. Mohamed E .Useful energy, economic and reduction of greenhouse gas emissions assessment of solar water heater and solar air heater for heating purposes in Gaza, Palestine[J].Heliyon,2023,9(6):e16803-e16803.
[28]. Dawei H ,Hengyu L ,Yidong Z , et al.Modeling and Simulation of Indirect Collector Solar Hot Water Heating System Based on TRNSYS[J].Journal of Physics: Conference Series,2023,2503(1):
[29]. Maria P ,Ian B ,Alessandro P , et al.Water-to-water heat pump integration in a solar seasonal storage system for space heating and domestic hot water production of a single-family house in a cold climate[J].Solar Energy,2021,213300-311.
[30]. Curtis M ,Ian B .Experimental and modelled performance of a building-scale solar thermal system with seasonal storage water tank[J].Solar Energy,2021,222145-159.
[31]. Beausoleil-Morrison I ,Kemery B ,Wills D A , et al.Design and simulated performance of a solar-thermal system employing seasonal storage for providing the majority of space heating and domestic hot water heating needs to a single-family house in a cold climate[J].Solar Energy,2019,19157-69.

Submitted: 17.08.2025.
Revised: 30.12.2025.
Accepted: 15.01.2026.